

Alveolar Epithelial Type II Cells Activate Alveolar Macrophages and Mitigate *P. Aeruginosa* Infection

Shibichakravarthy Kannan¹, Huang Huang¹, Drew Seeger¹, Aaron Audet¹, Yaoyu Chen², Canhua Huang³, Hongwei Gao¹, Shaoguang Li², Min Wu^{1,3*}

1 Department of Biochemistry and Molecular Biology, University of North Dakota, Grand Forks, North Dakota, United States of America, **2** Division of Hematology/Oncology, Department of Medicine, University of Massachusetts Medical School, Worcester, Massachusetts, United States of America, **3** State Key Laboratory for Biotherapy, West China Hospital, Sichuan University, Chengdu, China

Abstract

Although alveolar epithelial type II cells (AECII) perform substantial roles in the maintenance of alveolar integrity, the extent of their contributions to immune defense is poorly understood. Here, we demonstrate that AECII activates alveolar macrophages (AM) functions, such as phagocytosis using a conditioned medium from AECII infected by *P. aeruginosa*. AECII-derived chemokine MCP-1, a monocyte chemoattractant protein, was identified as a main factor in enhancing AM function. We proposed that the enhanced immune potency of AECII may play a critical role in alleviation of bacterial propagation and pneumonia. The ability of phagocytosis and superoxide release by AM was reduced by MCP-1 neutralizing antibodies. Furthermore, MCP-1^{-/-} mice showed an increased bacterial burden under PAO1 and PAK infection vs. wt littermates. AM from MCP-1^{-/-} mice also demonstrated less superoxide and impaired phagocytosis over the controls. In addition, AECII conditioned medium increased the host defense of airway in MCP-1^{-/-} mice through the activation of AM function. Mechanistically, we found that Lyn mediated NFκB activation led to increased gene expression and secretion of MCP-1. Consequently Lyn^{-/-} mice had reduced MCP-1 secretion and resulted in a decrease in superoxide and phagocytosis by AM. Collectively, our data indicate that AECII may serve as an immune booster for fighting bacterial infections, particularly in severe immunocompromised conditions.

Citation: Kannan S, Huang H, Seeger D, Audet A, Chen Y, et al. (2009) Alveolar Epithelial Type II Cells Activate Alveolar Macrophages and Mitigate *P. Aeruginosa* Infection. PLoS ONE 4(3): e4891. doi:10.1371/journal.pone.0004891

Editor: Jeffrey A. Gold, Oregon Health & Science University, United States of America

Received: December 30, 2008; **Accepted:** February 2, 2009; **Published:** March 23, 2009

Copyright: © 2009 Kannan et al. This is an open-access article distributed under the terms of the Creative Commons Attribution License, which permits unrestricted use, distribution, and reproduction in any medium, provided the original author and source are credited.

Funding: This work was supported by NIH ES014690 and P20 RR017699, American Heart Association Scientist Development Grant (National Office). The work is also supported by National Key Basic Research Program of China (973Program #2006CB504300). The funders had no role in study design, data collection and analysis, decision to publish, or preparation of the manuscript.

Competing Interests: The authors have declared that no competing interests exist.

* E-mail: minwu@medicine.nodak.edu

Introduction

Alveolar type II epithelial cells (AECII) maintain alveolar integrity by forming the alveolar barrier, producing surfactants and repairing injured type I epithelium [1]. Recently, several reports indicate that AECII may be an integral part of the lung innate immunity, acting to intensify the function of dendritic cells [2] and alveolar macrophages [3]. AECII may also perform other important functions such as cytokine secretion [4], antigen presentation [5] and enhancement of macrophage phagocytosis through surfactant proteins such as SP-D [6]. However, the role of AECII in infection immunity and underlying mechanism is largely unknown. Understanding the additional immunological role of AECII is important because professional immune cells such as alveolar macrophages (AM) in some cases rarely succeed in eradicating pathogens on their own. This is the case with *Pseudomonas aeruginosa*, an opportunistic gram-negative bacterium accounting for 10.1% of nosocomial infections. Clinical reports have shown that *P. aeruginosa* infects about 97.5% of Cystic Fibrosis children at age of 3 years [7]. *P. aeruginosa* infection is a main clinical problem in various immunodeficiency conditions such as HIV, severe burns, and cancers. This bacterium exhibits resistance to conventional antibiotics through a variety of virulence factors

and there are no effective vaccines, making it difficult to eradicate once it colonizes the respiratory tract [8,9].

Previous studies demonstrated that AECII cells can stimulate AM immunity in the lung of either mice or rats to boost the host defense against *P. aeruginosa* [4]. The caveats are that the studies have focused on whole animals to identify the cell types responsible for secreting chemokines by co-localization techniques. Also, the specific cell type involved in the immune activity has not been clearly defined. Although the main chemotactic factor released from AECII is likely to be MCP-1 [4], it is hard to prove *in vivo* whether AECII are the actual secreting cells. Also, the specific role of MCP-1 derived from AECII is less clear. A recent study suggested that isolated human AECII may secrete chemokines such as MCP-1 at higher amounts than AM primed with lipopolysaccharide (LPS) [10]. However, the specific immune response by characteristically defined AECII to *P. aeruginosa* infection remains to be determined. Furthermore, the underlying mechanism governing AECII mediated host immunity and regulatory factors involved in secretion of MCP-1 are not clearly established. Thus, it is necessary to investigate and fully establish the immune role of AECII.

To determine the immunological function of AECII, we chose to investigate if AECII have a role in activating AM in response to

P. aeruginosa infection. We used our primary cell culture models as well as mouse models including knockout mice to identify the signaling proteins that may regulate AM function and by identifying the cytokine products derived from AECII. We have shown here the importance of MCP-1 secreted by AECII in the activation of AM. Using MCP-1^{-/-} mice, we also confirmed that MCP-1 has a crucial activity in increasing AM functionality through enhancing phagocytosis, increasing superoxide production, balancing inflammatory response and thereby optimizing host defense. In addition, we delineated the mechanism that regulates MCP-1 secretion in AECII, in which we found that Lyn, a critical Src family member, can increase MCP-1 secretion by activating the NF- κ B pathway.

Results

Our objective was to test whether AECII in a culture system can boost the immune function of AM. Through co-culturing macrophages with lung epithelial cells, macrophages were significantly activated, demonstrating multiple functional activities including enhanced migration and actin reorganization (Figure S1A, B). To investigate whether secreted (soluble) substances are major mediators, we collected a conditioned medium from primary mouse AECII following PAO1 infection for 1 h and added to primary AM culture. After 24 h, AM activity was detected by three measurements: migration (Figure 1A), phagocytosis (Figure 1B) and superoxide production (Figure 1C). Our data indicates that the three AM function parameters were significantly increased by the AECII conditioned medium compared to the control medium from AECII without infection ($P < 0.05$, Student's *t* test). The activated AM also showed more significant morphological changes with membrane projections

such as lamellipodia and filopodia by confocal microscopy (Figure 1D). Moreover, we demonstrated apparent morphology alterations by scanning electron microscopy (SEM) (Figure 1E). Although we found that AECII have a role in activating AM, it is possible that AM themselves can be activated by *P. aeruginosa*, which enhances the function of resting AM through an autocrine loop. Thus, we evaluated whether the activated AM can bolster immunity by stimulating other naïve AM. We co-incubated resting AM with a conditioned medium that was derived from AM following *P. aeruginosa* time course infection. As expected, we have found that the AECII conditioned medium indeed showed greater increases in AM migration and superoxide production compared to the AM-conditioned medium, particularly at earlier times (6 h, Figure S1C). However, AM also secreted comparable MCP-1 possibly through autocrine activation at 24 h.

To investigate how AECII can activate AM, we studied the possible involvement of various cytokines and chemokines. Thus we performed an *in vitro* experiment with isolated primary mouse AECII to measure cytokines in the conditioned medium of AECII infected by *P. aeruginosa*, which showed a significant increase in MCP-1, IL-1 β , MIP-2 α , and TNF- α (Figure 2A, B). We also showed that MCP-1 can transmit cellular signals to AM (4), and may be a dominant cytokine in cultured AECII cells. The secretion of MCP-1 is time dependent (Figure 2B). Also, we detected increased expression of MCP-1 and CCR2 (MCP-1 receptor) expression on AECII cells by western blotting (Figure 2C). We further confirmed that the MCP-1-secreting cells expressed SP-C (a marker of AECII) by co-localization with confocal microscopy (Figure 2D). Similar results showing cytokine secretion by AECII were also found in murine lung type II cell line MLE-12 cells [11] (Figure S2A). We then infected mice to investigate MCP-1 secretion in response to *P. aeruginosa* infection in

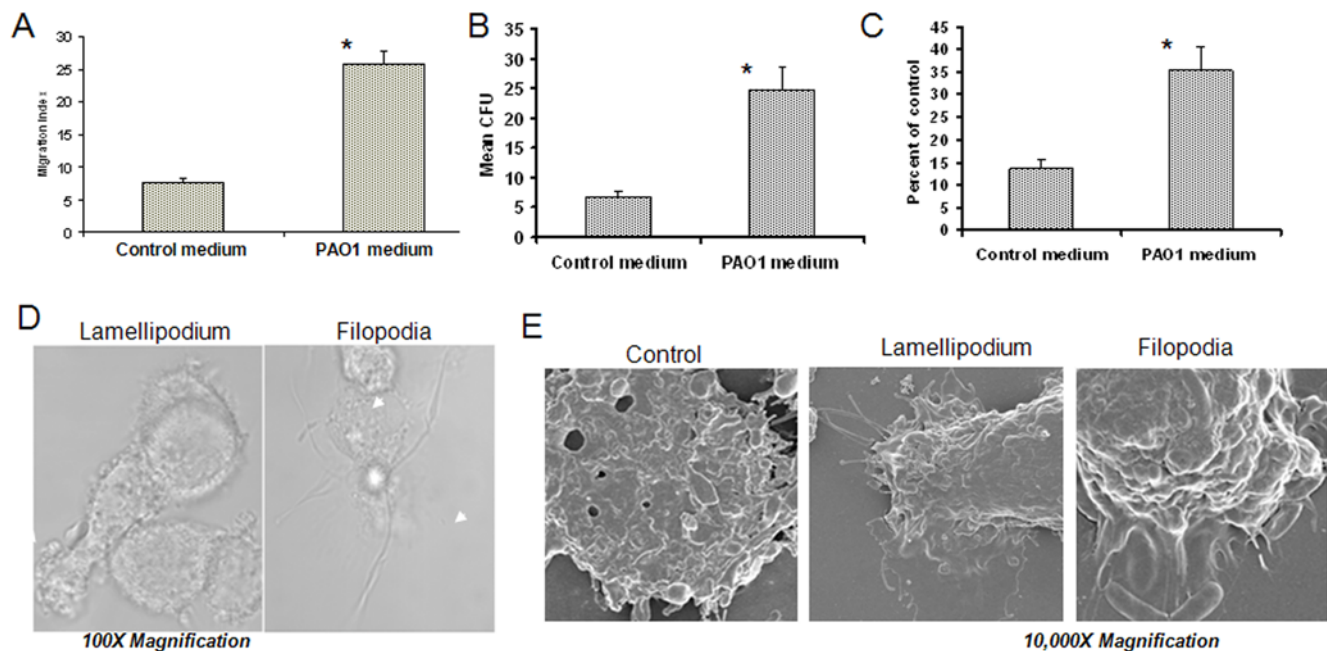


Figure 1. Conditioned medium from AECII by PAO1 infection activated AM (12 h). (A) Increase of AM migration as determined by chemotactic chamber methods (see Material and Methods). Migration index was calculated based on conditioned medium or control medium. (B) Increase in phagocytosis of AM as detected by CFU (colony forming units). (C) Increase in superoxide production of AM analyzed by H2DCF fluorescence (Molecular Probes). (D) The morphology of the activated AM is shown typically with lamellipodium and filopodium by confocal microscopy. (E) The morphology of the activated AM is further evidenced by high resolution and magnification Scanning Electron Microscopy (SEM). Statistical analysis was done by comparing mean individual values versus controls using student's *t* test, * $p < 0.05$ (95% Confidence Interval, CI). The results are representative of three experiments. doi:10.1371/journal.pone.0004891.g001

"*in vivo*" conditions [12]. C57BL6 mice (8 weeks female, 5 mice per group) were infected with PAO1 intranasally, and bronchoalveolar lavage (BAL) was performed 18 h post infection. MCP-1 level was found to be increased as measured by immunohistochemistry in lung tissue, and PAO1 infected mice showed a significant increase in MCP-1 compared to uninfected controls (Figure 2G). Furthermore, the MCP-1 expression was demonstrated on AECII cells of human lung tissues from CF patients with *P. aeruginosa* infection (Figure 2E), suggesting that MCP-1 actually participated in host defense in infected humans. We showed that lipid rafts in AECII are reorganized into aggregates (platforms for cell signaling) following acute infection by *P. aeruginosa* [12], which is consistent with several studies regarding *P. aeruginosa* or other microorganisms [13–15]. *P. aeruginosa* has three secretion system (T3SS) exoenzymes ExoS, ExoT, ExoU and ExoY, among which ExoS and ExoT are similar in the sequence and function for ADP ribosyltransferase and GTPase-activation

protein activities [16]. The raft aggregates are differentially induced by various T3SS mutants or a pili deficient mutant [12]. Since there were some rafts outside the *P. aeruginosa*, we further quantified raft aggregates using Image J software and showed that *P. aeruginosa* infection induced strong raft aggregates, which were also associated with *P. aeruginosa* (Figure 2F). In addition, controls without infection did not show raft aggregates, thus the aggregates of lipid rafts may be a specific response to *P. aeruginosa*. Next, we used various inhibitors to define the raft pathway in *P. aeruginosa* adhesion and internalization into AECII. Among the various inhibitors we have tested, we found that the lipid raft inhibitor (m β CD), Lyn tyrosine kinase inhibitor (PP2), Akt inhibitor, and NF- κ B inhibitor effectively blocked adhesion and internalization of *P. aeruginosa*, whereas the ceramide inhibitor (blocking sphingolipid pathway) only reduced internalization without affecting adhesion (Figure 2G, Table 1 and Figure S2B). This data suggests that ceramide and cholesterol may differentially

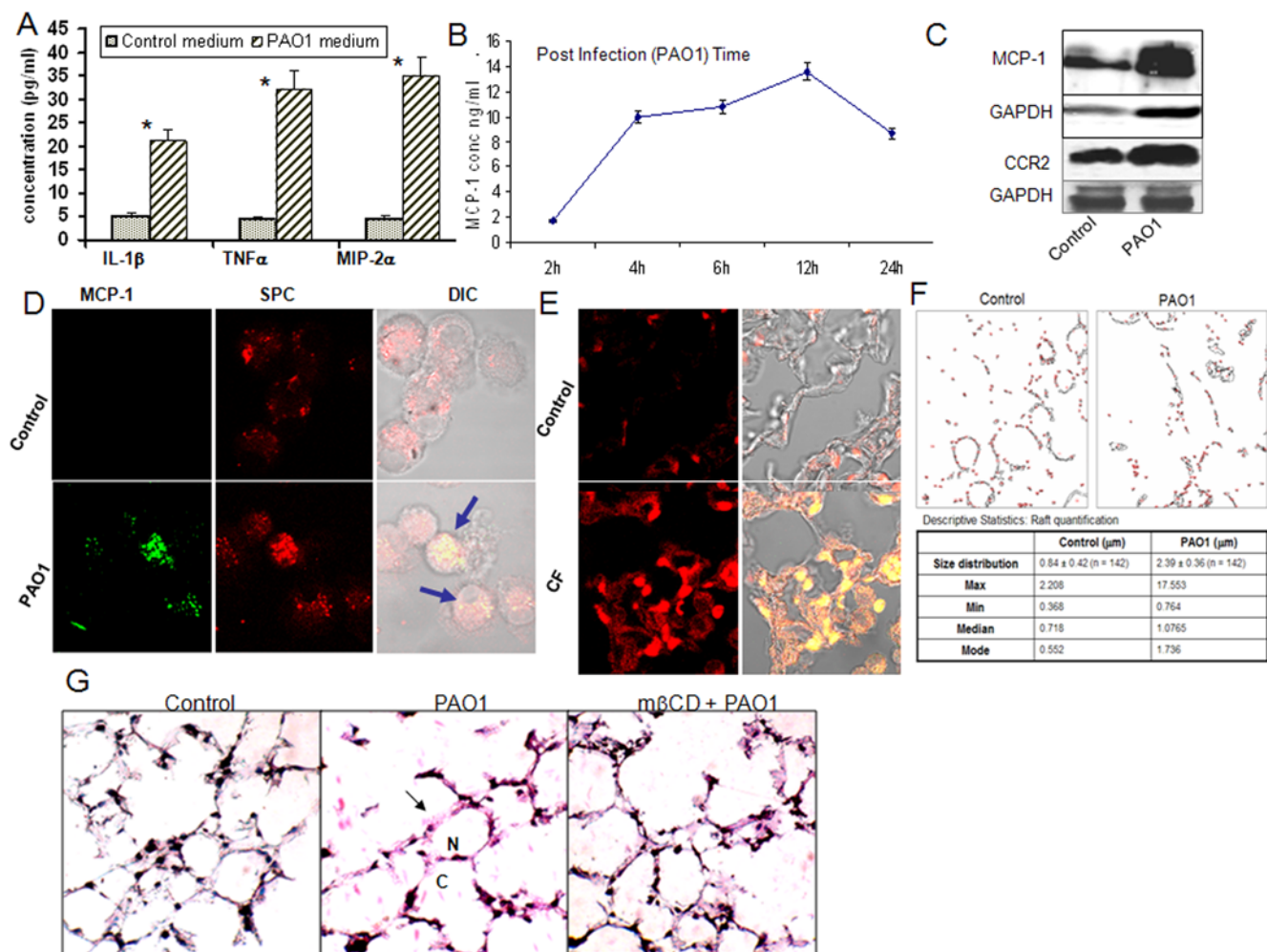


Figure 2. MCP-1 from AECII was a major regulator by PAO1 infection. (A) Increase of various proinflammatory factors at 24 h following stimulation with the conditioned medium from AECII infected by PAO1. (B) MCP-1 was significantly increased in a time dependent manner by the conditioned medium. (C) Both MCP-1 and its receptor of CCR2 were increased in AECII by PAO1 infection detected by western blotting. (D) Primary AECII secreted MCP-1 that was colocalized (arrows) with SP-C (a specific marker of AECII) as analyzed by immuno-fluorescence (anti-pro-SP-C from Dr. Jeffrey Whitsett). (E) Increase of MCP-1 expression in the AECII cells in human samples from Cystic Fibrosis (CF) patients (one of the 6 representative) stained by immunofluorescence. (F) Lipid raft quantification using Image J software. The colocalized pixels were identified and threshold defined vs. background. The image was converted into binary format and the "analyze particle tool" used to identify raft ranging in size of 15–255 pixels (correlates with 50–200 nm). (G) Blockade of lipid rafts with m β CD significantly reduced the secretion of MCP-1 in the lung vs. the control. The frozen sections for the lung tissue of C57BL6 mice (5 mice/group) were stained by anti-MCP-1 antibodies from Santa Cruz (arrows showing the positive staining). The results are representative of three experiments. doi:10.1371/journal.pone.0004891.g002

Table 1. Inhibition of adhesion and internalization of bacterium.

| Reagent | Adhesion | Internalization |
|--------------------|----------|-----------------|
| Control | 26 | 0.89 |
| m β CD | 2.2 | 0.07 |
| Ceramide inhibitor | 18 | 0.13 |
| PP2 | 4.2 | 0.28 |

*Raft blockers (m β CD cholesterol chelator, and ceramide inhibitor [Racemic] 3 mM Alexis) hampered PA internalization. PP2 is Lyn inhibitor.

doi:10.1371/journal.pone.0004891.t001

impact *P. aeruginosa* adhesion and internalization. To further dissect the mechanism, we intranasally instilled cholesterol chelator m β CD into mouse lungs and found a reduction in bacterial internalization and MCP-1 secretion was also partially hindered (Figure 2G).

The expression of CCR2 (MCP-1 receptor) was increased in AM treated with AECII conditioned medium as determined by

western blots (Figure 3A), indicating a functional involvement of this receptor in the pathway. Next, blocking of MCP-1 with neutralizing antibodies for 30 min before infection also down-regulated CCR2 compared to no antibody controls using fluorescent microscopy (Figure 3B). To further confirm the role of MCP-1, we added commercially available purified MCP-1 peptide (Calbiochem) directly to AM and found direct correlation between MCP-1 presence and AM activation, including superoxide production (Figure 3C). Furthermore, by blocking with MCP-1 neutralizing antibodies for 30 min before PAO1 infection, we observed that the mice showed more severe infection with increased bacterial burden (CFU/1 mg lung homogenates) compared to that in the wt mice (Figure 3D). In addition, the MCP-1 antibodies reduced superoxide production (Figure 3E) and phagocytosis by AM (Figure 3F) against the Ig isotype control. To ascertain the immune activity of AECII, we determined the immune symbolic markers, such as IL-12R and MHC Class II antigen by immunofluorescence. We showed that activated AECII expressed enhanced levels of MHC class II antigen as well as IL-12R and IL-17R (Figure S3A, B).

To further determine the role of MCP-1 as an immune stimulator, MCP-1 deficient mice (MCP-1^{-/-} mice) were used to

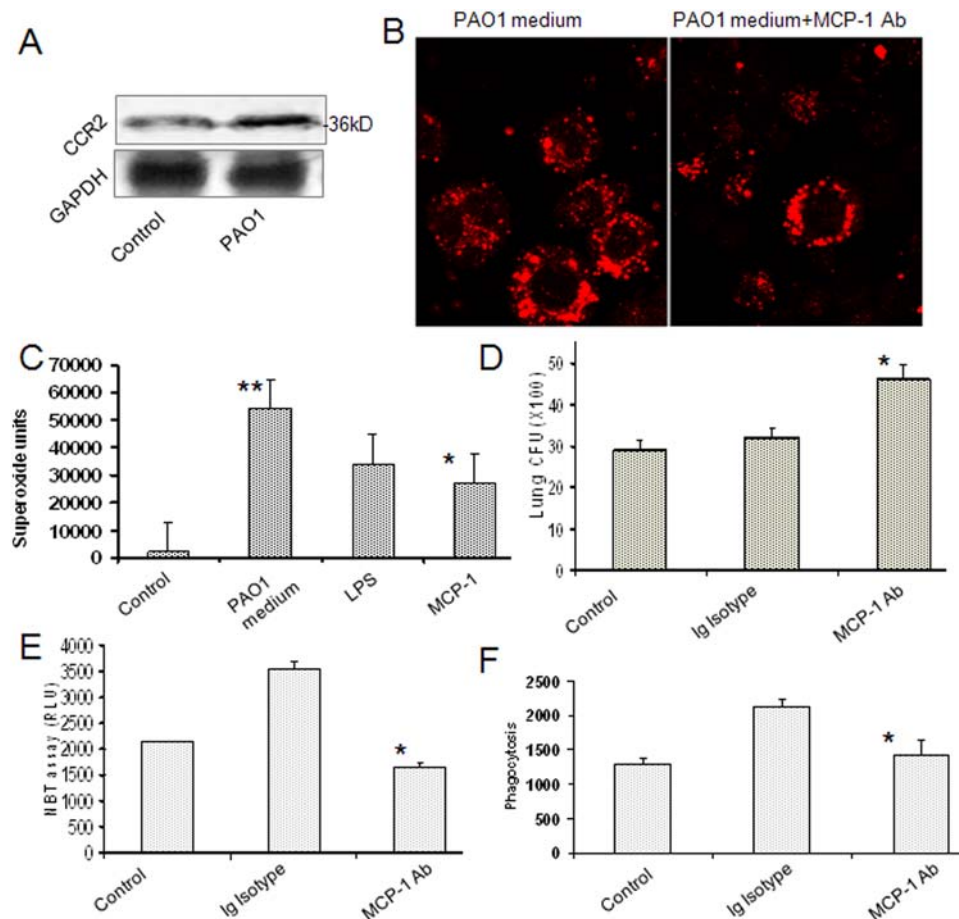


Figure 3. MCP-1 receptor was increased along the enhanced immune function and MCP-1 antibody alleviated the infection. (A) The receptor of MCP-1 (CCR2/CKR2) was also increased in AECII by PAO1 infection detected with western blotting. (B) CCR2 expression following PAO1 infection was reduced by pre-incubating with MCP-1 antibodies (30 min) and determined by immunofluorescence. (C) Increase in superoxide release was measured using H₂DCF by direct addition of the commercially available MCP-1 peptide. (D) BAL CFU from mice was increased by neutralizing antibodies against MCP-1 before PAO1 infection. (E) Superoxide was reduced in the AM from mice following instillation of MCP-1 antibodies as measured by NBT assay. (F) The AM from the same mice also demonstrated decreased phagocytosis ability. Statistical analysis was performed as above (** $p < 0.01$, 99% CI). The results are representative of three experiments. doi:10.1371/journal.pone.0004891.g003

study MCP-1 effects on AM immune function and physiological role during *P. aeruginosa* infection. This can also distinguish the relative contributions of MCP-1 to immune defense against *P. aeruginosa* infection. We found that MCP-1^{-/-} mice showed increased bacterial burden in the lung (Figure 4A). A significant decrease in the superoxide production in AM was also noted (Figure 4B). Furthermore, the lung from MCP-1^{-/-} mice showed increased lung cell death (showing decreased mitochondrial potential) following infection by *P. aeruginosa* (Figure 4C). Lung injury was also present as wet/dry ratio was increased by infection in the mice (data not shown). We also showed that isolated AM from MCP-1^{-/-} mice after bacterial infection had increased ability to phagocytose opsonized-*E. coli* particles (Figure 4D), indicating that the AM have not been saturated in uptaking bacteria (probably due to reduced migration) during *in vivo* infection. Interestingly, we noted that the lung injury is correlated

with the increase in a number of pro-inflammatory factors such as MIP-2 α (but probably also due to the loss of MCP-1) than the wild-type control (Figure 4E). Also, there was an increased neutrophil infiltration in the BAL (not shown). These data suggest that MCP-1 may be crucial in maintaining a fine balance between pro-inflammatory and anti-inflammatory cytokines, which is important for combating bacterial invasion as well as minimizing acute lung injury. Also, we instilled the conditioned medium into MCP-1^{-/-} mouse lungs, which increased the host defense compared to the control medium (Figure 4F). These data critically confirm that MCP-1 is a potent immune regulator and inflammation controller in the airway spaces.

Because raft signaling is partially dependent on T3SS, we attempted to define whether deletion in a single exoenzyme impacts the MCP-1 secretion by AECII. PAO1 wt and several toxin deficient strains (PAO1 Δ ExoS, Δ ExoT, PA14 Δ ExoU and

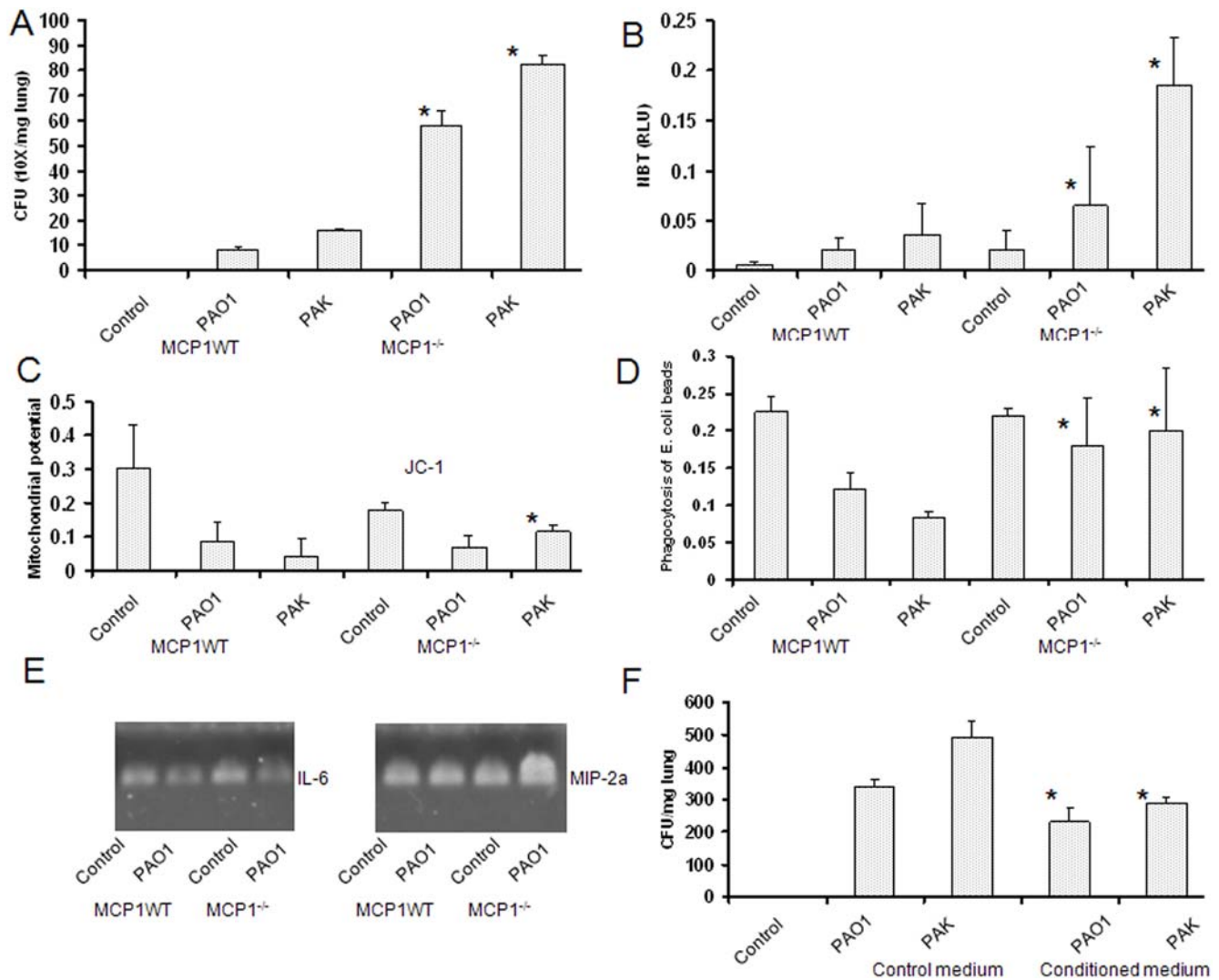


Figure 4. MCP-1^{-/-} mice demonstrated functional involvement with *P. aeruginosa* infection. (A) MCP-1^{-/-} mice showed more severe infection by *P. aeruginosa* (strains PAO1 and PAK) with an increase in bacterial burdens. Data were derived from a group of 5 infected and control mice (same in the figure). **(B)** Superoxide production was significantly altered in AM from MCP-1^{-/-} mice following infection identified by NBT assay. **(C)** A significant increase in apoptotic cell death was observed in MCP-1^{-/-} mice by bacterial infection. The data identified the loss of mitochondrial potential in MCP knockout mice, indicating increased cell apoptosis. **(D)** An increase opsonic phagocytosis with *E. coli* particles was found in AM derived from MCP-1^{-/-} mice following infection. **(E)** An increase in inflammatory chemokine MIP-2 α in the MCP-1^{-/-} mice after PAO1 infection. The mRNA expression is shown in an agarose gel using semi-quantitative RT-PCR. **(F)** Conditioned medium partially restored the immune defense against *P. aeruginosa* infection in MCP-1^{-/-} mice. Statistical analysis was as above. The results are representative of two experiments. doi:10.1371/journal.pone.0004891.g004

Δ ExoY) were employed to examine the effect on AECII cells. Our data indicates that the various T3SS mutant strains influenced secretion of MCP-1 compared to PAO1 wt (except Δ ExoT), the highest inducer being Δ ExoS as determined by RT-PCR and ELISA (Figure 5A, B). Consequently, the conditioned medium from mutant strain Δ ExoS induced greater AM activation (phagocytosis) than PAO1 wt (Figure 5C). By contrast, Δ ExoS strain resulted in lesser superoxide in AM than PAO1 wt strain (Figure 5D). One possible explanation for this result is that loss of a particular exoenzyme may reduce the bacterial invasive ability, permitting the host to mount a better defense. The controls with normal medium, DMSO (for inhibitor dilution) and PAO1 supernatant induce measurable but lesser response than that of live PAO1 (Figure 5D). We next examined whether live *P. aeruginosa* is necessary to induce MCP-1 secretion by AECII and to turn the cells immunologically more potent. Using dead PAO1 (heating at 60°C for 1 h), supernatant, LPS and live PAO1 wt (in the same amount of bacteria and same number of cells), we compared differences in MCP-1 secretion during infection of AECII. We found that live PAO1 increased MCP-1 secretion more so than did dead PAO1, supernatants, and LPS. The conditioned medium from live infection also induced the strongest activation of AM (Figure 5E). Thus, it is likely that live bacterial infection initiated stronger stimulation of AECII secretion than dead bacterium or its components.

Since Src tyrosine kinase Lyn is located in the inner cytoplasm membrane of the cell, in the general proximity to lipid rafts, we investigated the role of several members of this family and discovered that Lyn (p53/56) played a major role in *P. aeruginosa* infection. We have demonstrated that Lyn was activated in A549 cells following exposure to *P. aeruginosa* [12]. Lyn phosphorylation was measured by immunoblotting with phosphor-Src antibodies on immunoprecipitated Lyn protein from cell lysates. Pretreatment of AECII with 5 nM PP2 (synthetic inhibitor for Lyn) blocked MCP-1 secretion (Figure S2B).

To elaborate the role of Lyn in MCP-1 production, Lyn siRNA transfection was performed to assess the effect of Lyn on *P. aeruginosa* invasion (transfection efficiency >95%) [17], and our data show that MCP-1 was markedly decreased by Lyn siRNA (Figure 6A). Importantly, the role of Lyn was confirmed using Lyn^{-/-} mice, demonstrating significantly reduced MCP-1 by PAO1 and PAK infection vs. Lyn wt mice as determined by mRNA expression (Figure 6B). Reduction of MCP-1 secretion was also observed in Lyn^{-/-} mice as determined by ELISA (Figure 6C), while there is no difference between wt and KO mice in non-treated condition (data not shown). To probe downstream effectors in this pathway, we investigated NF- κ B activation in response to *P. aeruginosa* infection. We evaluated this signaling process and our data showed that blocking of Lyn using dominant negative transfection of LynK275D construct [12]

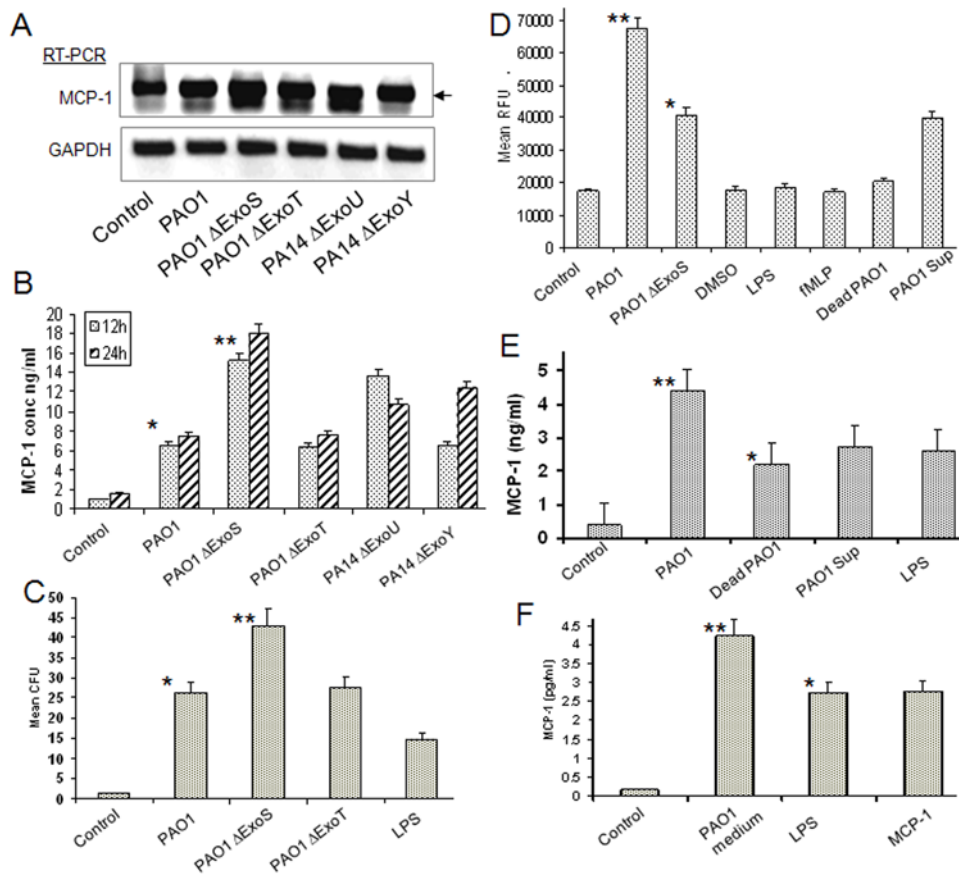


Figure 5. Exoenzymes were involved in MCP-1 secretion. (A) Δ ExoS strain induced increased MCP-1 mRNA and protein expression by MLE-12 lung epithelial cells assessed by RT-PCR and ELISA (B). (C) Δ ExoS strain resulted in increased phagocytosis by AM than PAO1 wt. (D) Δ ExoS strain induced decreased superoxide in AM (PAO1 sup: PAO1 supernatant; fMLP 5 μ M from Sigma). (E) Less potency by dead PAO1, PAO1 supernatant and LPS (*P. aeruginosa* lipopolysaccharide, serotype 10, 200 ng/ml, Sigma) in inducing MCP-1 than live PAO1. (F) MCP-1 alone also induced MCP-1 secretion in primary AECII. Statistical analysis was performed as above. The results are representative of two experiments. doi:10.1371/journal.pone.0004891.g005

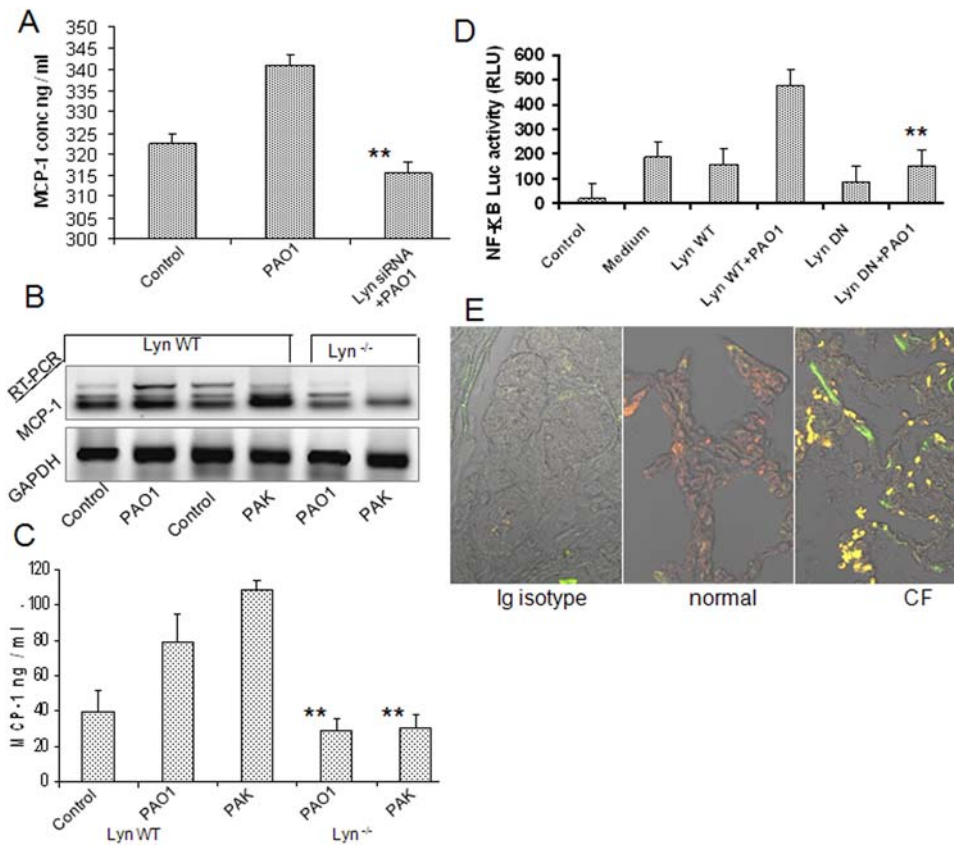


Figure 6. Lyn regulated MCP-1 production by activating NF- κ B. (A) MCP-1 secretion was abolished by Lyn siRNA transfection in AECII cells. (B) Decrease in MCP-1 expression in the lungs. (C) Decrease in MCP-1 expression secretion in BAL fluid (bronchoalveolar lavage) in Lyn^{-/-} mice by *P. aeruginosa* infection. Data were representative of two experiments with a group of 5 mice (infected and control). (D) Dominant negative Lyn construct transfection (DN=LynK275D) reduced NF- κ B translocation in AECII as determined by a Luciferase NF- κ B reporter assay. (E) Increased expression and activation of Lyn in human lung infected with *P. aeruginosa*. Tissues were from CF patients and normal controls (showing representative of 6 samples). Statistical analysis was done as above. The *in vitro* results are representative of three experiments. doi:10.1371/journal.pone.0004891.g006

significantly reduced the NF- κ B nuclear translocation compared to Lyn wt control transfectants (not shown). Using NF- κ B luciferase plasmid, we found a pronounced increase in luciferase activity with conditioned medium obtained from PAO1 infected AECII cells, but this was blocked by LynK275D transfection (Figure 6D). We also observed similar Lyn-K275D-based inhibition in functional roles of AM. These findings suggest that Lyn signaling is linked to both the secretion of AECII and its functional role of AM. Finally, we also demonstrated that Lyn overexpression and increased phosphorylation in the human lung tissue of CF patients against the normal control (Figure 6E). Our data indicate that Lyn activation might have occurred during CF disease process, thus it is reasonable to propose that Lyn may serve as a therapeutic target for controlling the disease.

The AECII – AM cross-talk is presented in a simplified model (Figure 7). Bacterial infection activates AECII cells that secrete chemokines (MCP-1). MCP-1 transmits signals to activate AM, which migrate towards infection sites and eliminate the pathogen. Lyn and lipid rafts may regulate MCP-1 and AM activation. In addition, the host defense may be balanced through the fine regulation by both Lyn and MCP-1.

Discussion

Previous reports, either from animal studies or from work with lung epithelial cells, indicate that epithelial cells can secrete

cytokines to increase AM immune function in combating *P. aeruginosa* infection [2,4]. Our studies use both isolated AECII mouse cells and animals (including knockout mice) and demonstrate that the chemokine MCP-1 can up-regulate the innate immunity of AM. Innate immunity of the respiratory system in normal individuals is sufficient to prevent *P. aeruginosa* infection, but is unable to eradicate the bacteria in immunodeficient individuals, resulting in recurrent infection or acute dissemination. Activating the immunological functions of AECII may lend much-needed help in fighting microorganisms such as *P. aeruginosa*. The results from our studies demonstrate that MCP-1 production was dramatically increased after infection of AECII. Further, we have shown that direct application of synthetic MCP-1 peptide also boosts AM functions, albeit in a less potent way compared to induction by *P. aeruginosa*-infected medium. In addition, the instillation of MCP-1-neutralizing antibodies into mouse lungs blocks cytokine secretion and induces more severe pneumonia, indicating a critical functional role of this particular chemokine. The foremost function of these secreted factors is to recruit AM and boost their microbicidal activity. Importantly, we show direct evidence from MCP-1 knockout mice, which exhibited reduced clearance of *P. aeruginosa* and increased pathological alterations in the lungs. In contrast, reconstitution of MCP-1 using conditioned medium partially recovered the inadvertent pathophysiology induced by *P. aeruginosa*.

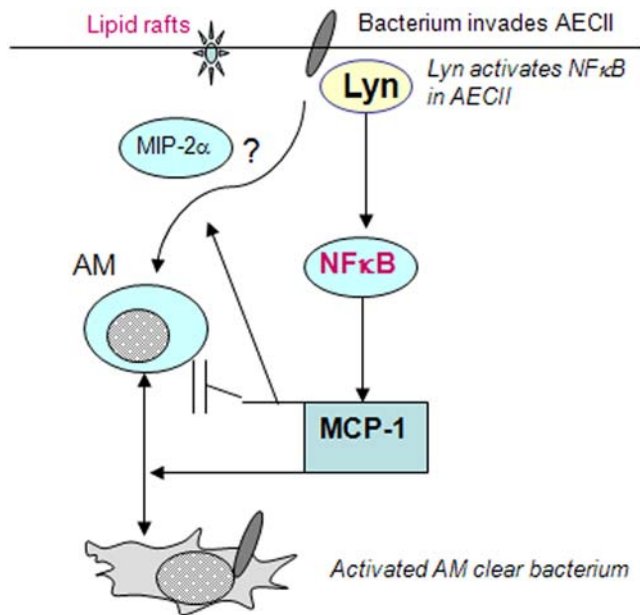


Figure 7. Diagram delineates a pathway involved in the AECII immune role against *P. aeruginosa* infection. AECII cells initiate an immunity to boost AM anti-infection function. The chemokine MCP-1 seems a crucial factor in this cell-cell cross-talk, which may be initiated by lipid rafts and regulated by Lyn. While boosting MCP-1 production through NF-κB pathway, Lyn may contain excessive production of MIP-2α as another mechanism to keep the inflammation response in control. doi:10.1371/journal.pone.0004891.g007

Lipid microdomains of cell surface make the platforms and initiate dynamics that directly or indirectly regulate the downstream activities, including cytokine secretion by AECII and bacterial phagocytosis by AM. We showed that lipid rafts in AECII are reorganized following acute infection by *P. aeruginosa* [12], which is consistent with several studies regarding *P. aeruginosa* or other microorganisms [13–15]. Thus we reasoned that AECII initial contact with the invading *P. aeruginosa* occurs through lipid rafts. Raft signaling may be beneficial to the host against *P. aeruginosa* [18], although some reports indicate that other pathogens (e.g., HIV) may use lipid rafts to subvert the innate immunity functions [19]. We also suggest that lipid rafts may directly associate the signaling pathway in activating AM [17]. Using ImageJ software, we provide quantitative evidence that lipid raft aggregates have a specific role in host defense against infection. Our data indicate that ceramide only associates with *P. aeruginosa* adhesion, while cholesterol impacts both adhesion and internalization to AECII cells. Our study also substantiates the role of lipid rafts in cytokine secretion, consistent with previous work in this field showing that TNF-α secretion is mediated by recruiting syntaxin-4 to lipid rafts [20]. Previous studies showed that various mechanisms such as JNK, TNF-α and IL1-β are implicated in boosting MCP-1 secretion [21].

Importantly, we have identified that Lyn is crucial in host defense against bacterial infections. Lyn up-regulates MCP-1 secretion and promotes AM activity. Although Lyn was previously shown to be involved in the progression of Friend virus-induced erythroleukemia [22], Lyn's role in secretion of cytokines is not known. We also showed that the Lyn mediated regulation of MCP-1 secretion may be through the activation of NF-κB, which is a key transcriptional factor for inducing gene expression of many immune molecules including MCP-1. Our data are consistent with a report from Kowalski et al [13], who showed that *P. aeruginosa*

infection of respiratory epithelial cells induced NF-κB nuclear translocation and blocking rafts using cholesterol chelating agents prevented this signaling. Lyn may also be able to increase reactive oxygen species production and release through the activation of PI3K and Akt [23–25] or other cellular signals (i.e., p47Phox, M.W., S.K., unpublished observations). Mechanistically, we identified a potential Lyn regulation site via H4 hyperacetylation at location K16 (unpublished). Additionally, we found that these responses may involve bacterial components including pili and ExoS. This is interesting because ExoS may be an important component of exoenzymes, responsible for intoxicating host defense mechanisms for bacterial benefit. In fact, pili as the surface structure of the bacterium may directly target lipid rafts to impact host signaling (not published). Also, reduction of MCP-1 production was seen when cells were challenged with a pili-deficient strain but increased MCP-1 secretion was noticed using the pili-corrected strain. Finally, our study also demonstrates that although dead bacteria or their partial products (LPS and supernatant) may have effects on igniting host defense, it is the live bacterium that stirred the strongest inflammatory response.

Whether or not AM are crucial for mitigating *P. aeruginosa* infection has been controversial. Our study has reaffirmed that AM are an important entity for exerting immune defense during acute *P. aeruginosa* infection. Our data indicates that activated AM are essential for phagocytosis of invading bacteria and scavenging dead bodies of neutrophils, evidenced by greater neutrophil penetration and pro-inflammatory cytokine response in Lyn^{-/-} mice. The increased superoxide in AECII-activated AM can be utilized to kill the engulfed bacteria, particularly important during high doses of bacterial infection. Our results indicate that AM alone may be less effective, while cytokines or chemokines derived from AECII or other unidentified mechanisms may give AM an added power that is required for clearance of invading microorganisms (Figure 7). However, the effects of AECII immune roles may impact other cell types such as neutrophils and lymphocytes, which may be interesting directions for future studies.

The Lyn axis maintains a fine balance involving several Src members or signaling proteins. Lyn through the ITAM motif up-regulates Syk function, which has been shown as important for opsonic phagocytosis by monocytes through FcγII mechanisms [26]. Lyn also has a positive role in ITIM motif that increases SH2 inositol phosphatase (SHIP), which may down-regulate inflammatory cytokines during acute infections [27–29]. Phagocytosis of the bacterium is dependent on many virulence factors as well as the host mediators. One of the major virulent effects of T3SS is disruption of cortical actin in phagocytic cells. We have reported earlier that a similar mechanism also exists in alveolar epithelium. Our recent study showed that T3SS is also involved in the phagocytosis of *P. aeruginosa* into AM [17]. *P. aeruginosa* releases these toxins directly into the host cytoplasm. Once activated, the ExoS and ExoT affect small GTPases by ADP ribosylation and GTPase activity, thereby deregulating cytoskeletal polymerization [30]. *P. aeruginosa* uses this mechanism to escape from phagocytosis and survive in the airways. Whether ExoS and ExoT have any direct effect on host cytokine secretion is less clear. Current studies demonstrate that secretion of MCP-1 may be inhibited by ExoS, as an ExoS-deficient strain induced even stronger secretion. Strain of ΔExoS also reduced superoxide release, but by an unknown mechanism.

Together, our study not only delineates the immunological role of AECII but also suggests that AM, aided by AECII, are important for combating *P. aeruginosa* infection. Specifically, we identified that the secreted MCP-1 was a major booster for AM

defense function and was regulated by Lyn. Furthermore, our data suggest that both Lyn and MCP-1 have crucial roles in balancing inflammatory response to bacterial challenge through interaction with various cell signaling proteins. The results from the current studies may open new avenues for the development of much-needed therapeutics for treating *P. aeruginosa* infection.

Methods

Animals. C57BL6 mice were purchased from the Jackson Laboratory. Lyn^{-/-} mice based on J129/C57BL6 mice (6–8 weeks, female and male) were as described previously [31,32]. MCP-1 mice were previously described [33], which were purchased from the Jackson Laboratory. The animal experiments have been approved by UND IACUC committee and were performed in accordance to the animal use and care guidelines. We anesthetized mice with 45 mg/kg ketamine plus 5 mg/kg diazepam, and intranasally instilled 0.1×10^7 (PAK) to 0.5×10^8 (PAO1) colony-forming units (CFUs) of *P. aeruginosa* for various times. After bronchoalveolar lavage (BAL), the trachea and lung were excised for homogenization or inflated with 50% OCT or formalin fixation. Intranasal instillation of the conditioned medium derived from *P. aeruginosa* infection with different bacterial strains was performed similarly as above. In selected experiments to check the efficiency of instillation, we used intratracheal instillation and ventilation procedures to confirm evenness of distribution in the lung.

Cell culture. Rat AECII cells were isolated as previously described and used within 2 days to preserve type II characteristics [12,34,35]. Mouse AM were isolated by bronchoalveolar lavage (BAL) concurrent to AECII isolation as described [17,36,37]. AECII cells were grown in Dulbecco's modified Eagle's medium (DMEM) and AM in RPMI 1640 medium supplemented with 10% newborn calf serum and penicillin/streptomycin antibiotics in 5% CO₂ incubator. A549, MLE-12 and MHS cells were obtained from ATCC and maintained following the manufacturer's instructions. For optimal seeding density, the cells were counted using Neubauer chamber and dead cells were excluded by the trypan blue exclusion assay. We generated and collected conditioned medium from primary mouse AECII following PAO1 infection for 1 h and cultured another 24 h (after adding 100 µg/ml polymycin to kill the surface bacteria). The control medium without infection was collected for use. After co-culturing primary AM with the conditioned medium for 24 h, AM activity was detected by functional measurements as described in the related sections.

Bacterial strains and infection. PAO1 wt is with an intact *pilC* gene and thus with twitching motility provided by Dr. S. Lory (Harvard) [38]. PAO1 wt GFP, *AfliC* (flagellin minus), Δ *exoS*, Δ *exoT* and Δ *exoU* deletion mutant strains, PAK (*pili* wt), PAK Δ *pilC* (*pili* deficient) and PAO1 were obtained from Dr. Gerald Pier (Harvard Medical School) [39]. PA14 wt (Δ *exoS*, Δ *exoT*, Δ *exoU* and Δ *exoY*) were from Dr. E. Drenkard (Massachusetts General Hospital) [40] and used in selected experiments. Bacteria were grown overnight in LB medium at 37°C without shaking. Absorbance at 600 nm was measured for quantification ($0.1 \text{ OD} = 1 \times 10^8$ bacterium/ml).

Immunohistochemistry and immunocytochemistry staining and confocal imaging. Adherent cells in Labtek chamber slides or animal/human tissue sections were stained for cell surface markers using appropriate primary antibodies and double stained for immunofluorescence with TRITC or FITC conjugated respective secondary antibodies. The cells were washed, and pictures taken with Zeiss LSM 510 confocal laser scanning

microscope (Carl Zeiss MicroImaging, Inc, Thornwood, NY). The human samples were used in accordance to the NIH exempt guidelines and approved by the UND IRB committee. For live cell imaging, MatTek glass bottom dishes were used with a portable incubation chamber to keep cells at 37°C.

RT-PCR analysis

RNA was extracted from Lung homogenates and cells with Trizol (Invitrogen Corporation) according to the manufacturer's instructions. For detected genes, reverse transcription (RT) was performed using 1.5 mg of RNA, RNase ribonuclease inhibitor, Oligo dT and cloned AMV reverse transcriptase (Invitrogen Corporation). cDNA was amplified using gene-specific primers as summarized in **Table 2**. PCR products were separated by 1.0% agarose gel electrophoresis containing ethidium bromide and visualized under UV light. The results for each gene were normalized in comparison with GAPDH expression.

Cytokine Immunoassay

Cytokine concentrations were measured by ELISA kit (eBioscience company) in cell culture medium, BAL fluid and lung homogenates collected at indicated times after infection. Briefly, the cells were treated as described as above. On 24 h or 48 h, culture mediums were collected and cells. For BAL fluid, the trachea was surgically exposed and cannulated, lungs were lavaged 5 times with 1.0 ml volumes of lavage fluid, the lavageates were pooled, and cells were removed by centrifugation. For lung homogenates, excised lungs were ground using a sterile glass-Teflon® in 500 µl PBS. 96-well plates (Corning Costar 9018) were coated with 100 µl/well of capture antibody in coating buffer and incubated overnight at 4°C. 100 µl aliquots of serum samples were added to the coated microtiter wells. The cytokine concentrations were determined with corresponding detection HRP-conjugated antibodies. The values were read at 450 nm and analyzed.

Western blot and Co-immunoprecipitation

The sample from cells and lung homogenates were lysed and quantitated. The lysates were boiled for 5 min, and protease inhibitors added. The supernatants were collected, and 30 µg of each sample were loaded onto 10% SDS-polyacrylamide mini-gels and electrophoresed to resolve proteins. The proteins were then transferred to polyvinylidene difluoride membranes (Pierce Biotechnology) and blocked overnight at 4°C using 5% non-fat milk blocking buffer western antibody buffer [41,42]. Membranes were incubated overnight at 4°C with the appropriate first antibodies diluted 1:1,000 in 5% non-fat milk blocking buffer. After washing three times with washing solution, the antigen-antibody complexes were incubated for 2 h at room temperature with horseradish peroxidase-conjugated secondary antibody

Table 2. Primers for cytokines.

| Gene | Sense | Antisense |
|-------|-------------------------|--------------------------|
| IL-6 | TTGCCCTCTTGGGACTGATGCT | GTATCTCTCTGAAGGACTCTGG |
| IFN-γ | TGCATCTTGGCTTGCAGCTCTTC | GGGTTGTTGACCTCAAACCTGGCA |
| TNF-α | ACCGTCAGCCGATTGCTATCTCA | TGGACATTCGAGGCTCCAGTGAAT |
| IRF-1 | CACCATGCCAATCACTCG | GGG TAG AGCTGCTGAGTCCA |
| MCP-1 | TCCCAATGAGTAGGCTGGAGAGC | CAGAAGGCTTGAAGTGGTTGTG |
| GAPDH | TAAAGGGCATCTGGGCTACACT | TTACTCTTGGAGGCCATGTAGG |

doi:10.1371/journal.pone.0004891.t002

(Amersham) diluted 1:2,000. Signals were visualized using enhanced chemiluminescence detection kit (SuperSignal West Pico; Pierce).

For co-immuno-precipitation, the supernatants were pre-cleared with bare protein A/G-Sepharose beads (Pierce) for 1 h at 4°C and then incubated with anti-MCP-1, anti-NFκB, or anti-Lyn Abs (Santa Cruz) bound to protein A/G Sepharose beads overnight at 4°C. The next day, beads were washed three times in lysis buffer and boiled in SDS sample loading buffer. The proteins were separated and analyzed by western blotting.

AM migration assay. AM migration was evaluated in either 8 μm transwell cell culture insert or chemotaxis chamber as described previously [43] using Boyden chamber. Briefly, cells were plated on the upper chamber and allowed to adhere overnight. After treatment, the filter was washed in phosphate buffered saline (PBS) and turned upside down; the migrated cells in the bottom of the filter were counted using specific red fluorescence (DiI, Molecular probes) staining followed by confocal microscopy. Cells were visualized by exciting with 533 nm wavelength HeNe laser and emission detected in the red spectra with a long pass filter. At least 100 fields per sample were counted for statistical purpose.

Fluorescent phagocytosis assay. AM cells were plated in 96 well plates and grown overnight. The cells were treated with the conditioned medium from AEC II for 2 h. Then FITC labeled *E. coli* or GFP PAO1 was used to infect the cells at MOI 1:10. After 1 h incubation at 37°C the wells were washed and treated with Polymixin 100 μg/ml for 1 hr to kill any remaining extracellular bacteria. The number of phagocytosed bacteria was counted using Synergy HT fluorimeter (BioTek) with 485±20 nm excitation and 528±20 emission filters. Background correction was done for autofluorescence.

Scanning electron microscopy (SEM). SEM was used to study morphology. AECII and AM cells were plated on collagen coated coverslips in 24-well plates. The cells were fixed in Karnovsky's fixative overnight, dehydrated by sequential alcohols, sputter coated with gold – palladium and images taken at 10000× magnification.

Lung edema. After infection, lungs were removed from the thoracic cavity, and the inferior third of the left lung were weighed and then placed in a drying oven at 90°C for 24 h. The specimen was reweighed, and the ratio of the weight before and after drying calculated.

Lipid peroxidation assay. Malondialdehyde (MDA) is an end product of lipid peroxidation process, and was measured in a colorimetric assay (Calbiochem, San Diego, CA) according to the manufacturer's instructions. Homogenized lung tissue in 62.5 mM Tris-HCL (pH = 6.8) supplemented with Complete-Mini Protease Inhibitor (Roche Diagnostics) in equal protein amounts were used in the assay.

Lung myeloperoxidase (MPO) assay. MPO assay was performed as described [44]. Samples were homogenized in 50 mM hexadecyltrimethylammonium bromide (HTAB) 50 mM KH₂PO₄, pH 6.0, and 0.5 mM EDTA, 1 mL/100 mg tissue and centrifuged for 15 min at 12000 rpm at 4°C. Supernatants were decanted and 100 μl of reaction buffer (0.167 mg/mL *O*-dianisidine, 50 mM KH₂PO₄, pH 6.0 and 0.0005% mM H₂O₂) was added to 100 μl sample. Absorbance was read at 460 nm at 2 min intervals.

H2DCF Assay for Superoxide production. H2DCF dye (Molecular Probes) does not normally fluoresce and emits green fluorescence upon reaction with superoxide inside cells[45]. Cells were treated as above and equal amount(s) of dye added. Fluorescence was measured after 10 min incubation using the

fluorimeter (BioTek, in our laboratory). For confirmation, NBT assay was used as we described previously [17].

siRNA. A pool of four specific siRNAs or sense controls was ('A pool' is singular) purchased from Dharmacon (West Lafayette, Colorado) to deplete Lyn in MLE-12, AECII and MSH cells and the depleted expression assessed as we previously described [17].

Statistical analyses. Comparison of test with controls was done in triplicates and the results were analyzed using two tailed Student's *t* test with a P value<0.05. For multiple groups with an equal variance, we performed one-way ANOVA. For analyzing image data the sample size was increased by taking pictures of at least 100 cells per sample.

Supporting Information

Figure S1 AECII cells activate macrophages after PAO1 infection. Actin polymerization was induced by the medium from A549 cells infected by PAO1 in the Boyden chamber, which has two compartments separated by a porous membrane. RAW264 cells were seeded in the top and A549 cells in the bottom. Infection of A549 cells was done separately before inoculation into the chamber. Migrating cells were identified by staining the porous membrane with rhodamine phalloidin for actin and DAPI for nucleus and images taken by Zeiss confocal microscope. RAW264 cells started migrating towards infected A549 cells within 30 min (A). Quantification of actin cytoskeletal changes in RAW264 cells upon infection (B). RAW264 cells were grown on coverslips in 24 well plate. Cells were infected with PAO1 at 1:10 ratio for 1 h. The cells were fixed in 4% PFA and stained with FITC CT (Lipid raft marker) and Rhodamine Phalloidin (Actin). Untreated controls showed more number of cells (52%) with cytoskeletal changes like lamellipodium formation. The graph shows percent positive for cytoskeletal changes and error bar denotes standard deviation (P<0.01). AM conditioned medium has less potential for attracting AM than the conditioned medium from AECII by determining the migration index (C). Percentage of the migration of treated samples against total cells counted.

Found at: doi:10.1371/journal.pone.0004891.s001 (1.33 MB TIF)

Figure S2 MCP-1 secreted by MLE-12 or isolated AECII is a major chemokine by PAO1 infection. MCP-1 expression is induced in MLE-12 cells by PAO1 infection. Lyn siRNA and various inhibitors (PP2 and Rac1 inhibitor, Calbiochem) decrease the expression of MCP-1 (A). AM under infection show less secretion of MCP-1 than AECII cells. Also, additional inhibitors examined demonstrate inhibition of MCP-1 expression in AM and AECII cells. In addition, co-culturing of AM with AECII induces increased secretion of MCP-1 than either cell alone (B).

Found at: doi:10.1371/journal.pone.0004891.s002 (1.16 MB TIF)

Figure S3 Activated AECII demonstrate increased immunological characteristics including class II expression under PAO1 infection (A). Immunological markers including IL-12R (FITC) and IL-17R (TRITC) are increased against controls (not shown) under PAO1 infection (B) (all antibodies obtained from Santa Cruz).

Found at: doi:10.1371/journal.pone.0004891.s003 (1.59 MB TIF)

Acknowledgments

We would like to thank Drs. Gerald Pier, Stephen Lory, Joseph T Barbieri, and Eliana Drenkard for providing various PA strains and Dr. Thomas Smithgall for Lyn's constructs. We thank Dr. S. Pierce of NIAID for kindly providing us with the Lyn-YFP construct and Dr. O Miura of Tokyo Medical and Dental University for GST Lyn plasmids. We thank B. Grove, A. Eberhardt, S. Rolling, and D. Laturnus in UND imaging core for help with confocal and SEM imaging. We are indebted to Dr. Scott Randell for providing human tissue sections.

Author Contributions

Conceived and designed the experiments: SK HG MW. Performed the experiments: SK HH DS AA. Analyzed the data: SK SL MW.

Contributed reagents/materials/analysis tools: YC CH SL. Wrote the paper: SK MW.

References

- Fehrenbach H (2001) Alveolar epithelial type II cell: defender of the alveolus revisited. *Respir Res* 2: 33–46.
- Thorley AJ, Goldstraw P, Young A, Tetley TD (2005) Primary human alveolar type II epithelial cell CCL20 (macrophage inflammatory protein-3 α)-induced dendritic cell migration. *Am J Respir Cell Mol Biol* 32: 262–267.
- Sato K, Tomioka H, Shimizu T, Gonda T, Ota F, et al. (2002) Type II alveolar cells play roles in macrophage-mediated host innate resistance to pulmonary mycobacterial infections by producing proinflammatory cytokines. *J Infect Dis* 185: 1139–1147.
- Amano H, Morimoto K, Senba M, Wang H, Ishida Y, et al. (2004) Essential contribution of monocyte chemoattractant protein-1/C-C chemokine ligand-2 to resolution and repair processes in acute bacterial pneumonia. *J Immunol* 172: 398–409.
- Lo B, Hansen S, Evans K, Heath JK, Wright JR (2008) Alveolar epithelial type II cells induce T cell tolerance to specific antigen. *J Immunol* 180: 881–888.
- Restrepo CI, Dong Q, Savov J, Mariencheck WI, Wright JR (1999) Surfactant protein D stimulates phagocytosis of *Pseudomonas aeruginosa* by alveolar macrophages. *Am J Respir Cell Mol Biol* 21: 576–585.
- Burns JL, Gibson RL, McNamara S, Yim D, Emerson J, et al. (2001) Longitudinal assessment of *Pseudomonas aeruginosa* in young children with cystic fibrosis. *J Infect Dis* 183: 444–452.
- LeVine AM, Kurak KE, Bruno MD, Stark JM, Whitsett JA, et al. (1998) Surfactant protein-A-deficient mice are susceptible to *Pseudomonas aeruginosa* infection. *Am J Respir Cell Mol Biol* 19: 700–708.
- Mariencheck WI, Savov J, Dong Q, Tino MJ, Wright JR (1999) Surfactant protein A enhances alveolar macrophage phagocytosis of a live, mucoid strain of *P. aeruginosa*. *Am J Physiol* 277: L777–786.
- Thorley AJ, Ford PA, Gienbycz MA, Goldstraw P, Young A, et al. (2007) Differential regulation of cytokine release and leukocyte migration by lipopolysaccharide-stimulated primary human lung alveolar type II epithelial cells and macrophages. *J Immunol* 178: 463–473.
- Das A, Boggaram V (2007) Proteasome dysfunction inhibits surfactant protein gene expression in lung epithelial cells: mechanism of inhibition of SP-B gene expression. *Am J Physiol Lung Cell Mol Physiol* 292: L74–84.
- Kannan S, Audet A, Knittel J, Mullegama S, Gao GF, et al. (2006) Src kinase Lyn is crucial for *Pseudomonas aeruginosa* internalization into lung cells. *European J Immunol* 36: 1739–1752.
- Kowalski MP, Pier GB (2004) Localization of cystic fibrosis transmembrane conductance regulator to lipid rafts of epithelial cells is required for *Pseudomonas aeruginosa*-induced cellular activation. *J Immunol* 172: 418–425.
- Soong G, Reddy B, Sokol S, Adamo R, Prince A (2004) TLR2 is mobilized into an apical lipid raft receptor complex to signal infection in airway epithelial cells. *J Clin Invest* 113: 1482–1489.
- Zaas D, Duncan M, Li G, Wright JR, Abraham SN (2005) *Pseudomonas* invasion of type I pneumocytes is dependent on the expression and phosphorylation of caveolin-2. *J Biol Chem* 280: 4864–4872.
- Hauser AR, Engel JN (1999) *Pseudomonas aeruginosa* induces type-III-secretion-mediated apoptosis of macrophages and epithelial cells. *Infect Immun* 67: 5530–5537.
- Kannan S, Audet A, Huang H, Chen LJ, Wu M (2008) Cholesterol-Rich Membrane Rafts and Lyn Are Involved in Phagocytosis during *Pseudomonas aeruginosa* Infection. *J Immunol* 180: 2396–2408.
- Grassme H, Jendrosseck V, Riehle A, von Kurthy G, Berger J, et al. (2003) Host defense against *Pseudomonas aeruginosa* requires ceramide-rich membrane rafts. *Nat Med* 9: 322–330.
- Lafont F, Abrami L, van der Goot FG (2004) Bacterial subversion of lipid rafts. *Curr Opin Microbiol* 7: 4–10.
- Kay JG, Murray RZ, Pagan JK, Stow JL (2006) Cytokine secretion via cholesterol-rich lipid raft-associated SNAREs at the phagocytic cup. *J Biol Chem* 281: 11949–11954.
- Zhou Y, Ling EA, Dheen ST (2007) Dexamethasone suppresses monocyte chemoattractant protein-1 production via mitogen activated protein kinase phosphatase-1 dependent inhibition of Jun N-terminal kinase and p38 mitogen-activated protein kinase in activated rat microglia. *J Neurochem* 102: 667–678.
- Subramanian A, Hegde S, Correll PH, Paulson RF (2006) Mutation of the Lyn tyrosine kinase delays the progression of Friend virus induced erythroleukemia without affecting susceptibility. *Leuk Res* 30: 1141–1149.
- Zhu QS, Xia L, Mills GB, Lowell CA, Touw IP, et al. (2006) G-CSF induced reactive oxygen species involves Lyn-PI3-kinase-Akt and contributes to myeloid cell growth. *Blood* 107: 1847–1856.
- Kierbel A, Gassama-Diagne A, Mostov K, Engel JN (2005) The phosphoinositide-3-kinase-protein kinase B/Akt pathway is critical for *Pseudomonas aeruginosa* strain PAK internalization. *Mol Biol Cell* 16: 2577–2585.
- Hoyal CR, Gutierrez A, Young BM, Catz SD, Lin JH, et al. (2003) Modulation of p47PHOX activity by site-specific phosphorylation: Akt-dependent activation of the NADPH oxidase. *Proc Natl Acad Sci U S A* 100: 5130–5135.
- Fitzer-Attas CJ, Lowry M, Crowley MT, Finn AJ, Meng F, et al. (2000) Fc γ receptor-mediated phagocytosis in macrophages lacking the Src family tyrosine kinases *Hck*, *Fgr*, and *Lyn*. *J Exp Med* 191: 669–682.
- Neff TA, Guo RF, Neff SB, Sarma JV, Speyer CL, et al. (2005) Relationship of acute lung inflammatory injury to Fas/FasL system. *Am J Pathol* 166: 685–694.
- Baran CP, Tridandapani S, Helgason CD, Humphries RK, Krystal G, et al. (2003) The inositol 5'-phosphatase SHIP-1 and the Src kinase Lyn negatively regulate macrophage colony-stimulating factor-induced Akt activity. *J Biol Chem* 278: 38628–38636.
- Kamen LA, Levinsohn J, Cadwallader A, Tridandapani S, Swanson JA (2008) SHIP-1 increases early oxidative burst and regulates phagosome maturation in macrophages. *J Immunol* 180: 7497–7505.
- Maresco AW, Baldwin MR, Barbieri JT (2004) Ezrin/radixin/moesin proteins are high affinity targets for ADP-ribosylation by *Pseudomonas aeruginosa* ExoS. *J Biol Chem* 279: 38402–38408.
- Chan VW, Meng F, Soriano P, DeFranco AL, Lowell CA (1997) Characterization of the B lymphocyte populations in Lyn-deficient mice and the role of Lyn in signal initiation and down-regulation. *Immunity* 7: 69–81.
- Hu Y, Liu Y, Pelletier S, Buchdunger E, Warmuth M, et al. (2004) Requirement of Src kinases Lyn, *Hck* and *Fgr* for BCR-ABL1-induced B-lymphoblastic leukemia but not chronic myeloid leukemia. *Nat Genet* 36: 453–461.
- Lu B, Rutledge BJ, Gu L, Fiorillo J, Lukacs NW, et al. (1998) Abnormalities in monocyte recruitment and cytokine expression in monocyte chemoattractant protein 1-deficient mice. *J Exp Med* 187: 601–608.
- Dobbs LG (1990) Isolation and culture of alveolar type II cells. *Am J Physiol Lung Cell Mol Physiol* 258: L134–147.
- Kannan S, Pang H, Foster D, Rao Z, Wu M (2006) Human 8-oxoguanine DNA glycosylase links MAPK activation to resistance to hyperoxia in lung epithelial cells. *Cell Death Differ* 13: 311–323.
- Wu M, Hussain S, He HY, Pasula R, Smith PA, et al. (2001) Genetically engineered macrophages expressing IFN- γ restore alveolar immune function in *scid* mice. *Proc Natl Acad Sci U S A* 98: 14589–14594.
- Wisniewski PE, Speck RW, Wu M, Doyle NA, Pasula R, et al. (2000) Vitronectin protects alveolar macrophages from silica toxicity. *Am J Respir Crit Care Med* 162: 733–739.
- Stare CK, Pham XQ, Erwin AL, Mizoguchi SD, Warrener P, et al. (2000) Complete genome sequence of *Pseudomonas aeruginosa* PA01, an opportunistic pathogen. *Nature* 406: 959–964.
- Preston MJ, Seed PC, Toder DS, Iglewski BH, Ohman DE, et al. (1997) Contribution of proteases and LasR to the virulence of *Pseudomonas aeruginosa* during corneal infections. *Infect Immun* 65: 3086–3090.
- Miyata S, Casey M, Frank DW, Ausubel FM, Drenkard E (2003) Use of the *Galleria mellonella* caterpillar as a model host to study the role of the type III secretion system in *Pseudomonas aeruginosa* pathogenesis. *Infect Immun* 71: 2404–2013.
- Wu M, Brown WL, Stockley PG (1995) Cell-specific delivery of bacteriophage-encapsidated ricin A chain. *Bioconjugate Chem* 6: 587–595.
- Wu M, Stockley PG, Martin II WJ (2002) An improved Western blotting effectively reduces the background. *Electrophoresis* 23: 2373–2376.
- O'Brien AD, Standiford TJ, Christensen PJ, Wilcoxon SE, Paine Rr (1998) Chemotaxis of alveolar macrophages in response to signals derived from alveolar epithelial cells. *J Lab Clin Med* 131: 391–392.
- Drannik AG, Pouladi MA, Robbins CS, Goncharova SI, Kianpour S, et al. (2004) Impact of cigarette smoke on clearance and inflammation after *Pseudomonas aeruginosa* infection. *Am J Respir Crit Care Med* 170: 1164–1171.
- Steinhauser ML, Hogaboam CM, Kunkel SL, Lukacs NW, Strieter RM, et al. (1999) IL-10 is a major mediator of sepsis-induced impairment in lung antibacterial host defense. *J Immunol* 162: 392–399.